CrossMark

*J. Appl. Prob.* **58,** 677–692 (2021)
*doi:*10.1017/jpr.2020.111

# AN UPPER BOUND FOR THE BOND PERCOLATION THRESHOLD OF THE CUBIC LATTICE BY A GROWTH PROCESS APPROACH

GAORAN YU,* ** AND
JOHN C. WIERMAN,* *** *Johns Hopkins University*

**Abstract**

We reduce the upper bound for the bond percolation threshold of the cubic lattice from 0.447 792 to 0.347 297. The bound is obtained by a growth process approach which views the open cluster of a bond percolation model as a dynamic process. A three-dimensional dynamic process on the cubic lattice is constructed and then projected onto a carefully chosen plane to obtain a two-dimensional dynamic process on a triangular lattice. We compare the bond percolation models on the cubic lattice and their projections, and demonstrate that the bond percolation threshold of the cubic lattice is no greater than that of the triangular lattice. Applying the approach to the body-centered cubic lattice yields an upper bound of 0.292 893 for its bond percolation threshold.

*Keywords:* Bond percolation; percolation threshold; cubic lattice; body-centered cubic lattice; projection

2010 Mathematics Subject Classification: Primary 60K35
Secondary 05C80; 82B43

## 1. Introduction

Mathematical percolation theory studies the connected components of infinite random graphs. One major concern in percolation theory is the derivation of bond percolation thresholds. There are two families of two-dimensional lattices for which the bond percolation thresholds can be exactly determined: Solution methods by [24, 36, 49, 53–55] apply to an infinite class of lattices, including square, triangular, hexagonal, bow-tie, and martini lattices, which may be constructed by embedding generator graphs in self-dual 3-uniform hypergraphs. Exact solutions may also be derived for isoradial graphs [19].

Since the percolation thresholds of very few lattices are exactly known, there is widespread interest in approximating the value of the percolation thresholds of various lattices. Numerous simulation estimates of percolation thresholds are computed for the physical sciences literature each year, involving applications to, for example, polymer nanocomposites [13], carbon nanotubes [11], hydrogen-bonded water clusters [22], diffusivity of porous media [25], epidemic processes [2], and cementitious materials [31].

Various methodologies have been developed to bound percolation thresholds in cases where they cannot be determined exactly (see [5, 18, 27, 28, 43–47]). Besides being a

Received 15 November 2018; revision received 23 November 2020.
* Postal address: Department of Applied Mathematics and Statistics, Wyman Park Building, Fourth Floor, Johns Hopkins University, 3400 N Charles Street, Baltimore, MD 21218, USA.
** Email address: gyu9@jhu.edu
*** Email address: jwierma1@jhu.edu

© The Author(s), 2021. Published by Cambridge University Press on behalf of Applied Probability Trust.



https://doi.org/10.1017/jpr.2020.111 Published online by Cambridge University Press

mathematically challenging problem, research on bounds potentially develops techniques which may eventually lead to exact solutions, as it did for the square lattice bond percolation model. Mathematically rigorous bounds have become increasingly accurate, recently providing three-digit accuracy for the $(3, 12^2)$ lattice [48] and two-digit accuracy for the kagome lattice [50], disproving long-standing conjectured exact values [37]. Percolation threshold bounds are also applied in the study of related models. As examples, Cotar, Holroyd, and Revelle [7] used an upper bound for the hexagonal lattice site percolation threshold [28] to prove the existence of percolation in a Poisson hard sphere process, and Don [12] used a lower bound for the square lattice site percolation threshold [38] to produce a bound for the threshold of fractal percolation.

In this article we focus on the percolation thresholds of two three-dimensional lattices. Currently, none of the bond percolation thresholds of three-dimensional lattices have been exactly determined. Moreover, there are few rigorous upper and lower bounds, and those that exist are not very accurate.

For a comprehensive discussion of percolation theory, see [4, 17, 21].

## 1.1. The cubic lattice

The cubic lattice bond model is the most well-studied three-dimensional bond percolation model. Denote the canonical embedding of the cubic lattice by $\mathbb{L}^3 = (\mathbb{Z}^3, \mathbb{E}^3)$, where $\mathbb{Z}^3$ are points in $\mathbb{R}^3$ with integer coordinates and $\mathbb{E}^3$ are pairs of points in $\mathbb{Z}^3$ whose Euclidean distance is 1. Let $p_c(\mathbb{L}^3)$ denote the bond percolation threshold of $\mathbb{L}^3$. Before 1990, there were extensive Monte Carlo simulations [15, 20, 35, 40, 51], series expansion approximations [1, 14, 36], and renormalization estimates [10, 30, 32] for $p_c(\mathbb{L}^3)$ ranging from 0.209 to 0.254. Since 1990, with more advanced algorithms and increased computing power, simulation results are consistently in the range $0.2488 \pm 0.0001$ [8, 16, 26, 34, 39, 41], with the most recent estimates clustered near 0.248 812 [8, 26, 41].

As for rigorous bounds for $p_c(\mathbb{L}^3)$, in 1985 Campanino and Russo [6] proved that the site percolation threshold of $\mathbb{L}^3$ is strictly less than 0.5, which implies that $p_c(\mathbb{L}^3) < 0.5$. The smallest previous upper bound, 0.447 792, was proved using the containment principle and substitution method [47], while the largest lower bound is 0.209 082, which follows from self-avoiding walk enumeration [33].

Letting $\mathbb{T}$ denote the planar triangular lattice, our principal result is the following:

**Theorem 1.** *For bond percolation models,* $p_c(\mathbb{Z}^3) \le p_c(\mathbb{T})$.

For comparison with the previous upper bound of 0.447 792, note that $p_c(\mathbb{T}) = 2\sin(\pi/18) = 0.347\,296\ldots$ (see [42]).

## 1.2. The growth process approach for the cubic lattice

For each configuration of a random graph, its open cluster is the set of all vertices connected to a prespecified vertex through open edges. The core idea of the growth process approach is that we no longer consider the open cluster to be a static collection of vertices, but a dynamically growing process. This approach is inspired by a method introduced in [29] to analyze site percolation models with multiple states. (The standard site percolation model is a random designation of two states, open or closed, for each vertex of the lattice.) Their method was modified by [38] to provide a rigorous lower bound for the percolation threshold of the square lattice site model. The growth process approach refers to this idea and generalizes it to analyze the bond percolation model on the cubic lattice.

https://doi.org/10.1017/jpr.2020.111 Published online by Cambridge University Press

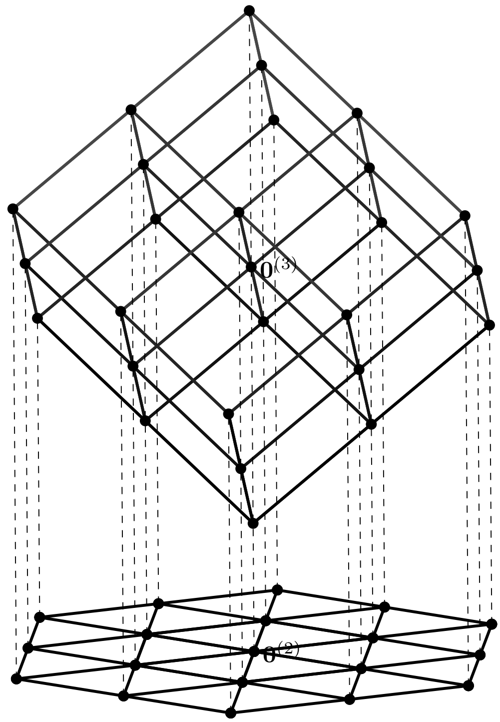


FIGURE 1. An illustration of the rotated cubic lattice $\mathbb{L}^3 \cdot R$ and its projection onto $\mathbb{R}^2$, which is the triangular lattice $\mathbb{T}$.

Note that our growth process approach has similarities to that in [3, Theorem 1], which is stated for site percolation models but is readily adapted to bond percolation models. However, there are important differences between the two approaches in our context. We consider it more natural and intuitive to explore in three dimensions and project to construct a two-dimensional open cluster, while [3] explores in two dimensions and constructs a three-dimensional open cluster. Since [3] associates a single edge in the three-dimensional lattice with an edge in the two-dimensional lattice, their approach produces an upper bound equal to the percolation threshold of the two-dimensional lattice. While both methods derive the same upper bound for the simple cubic lattice, our approach provides a smaller upper bound for the body-centered cubic lattice (see Section 3). Our approach also generalizes to the face-centered cubic lattice and stacked lattices, obtaining smaller upper bounds than the approach in [3] would provide (see [52] for details).

Note also that a different dynamic growth process approach has been used to study the chemical distance in percolation models. The *chemical distance* between two vertices $x$ and $y$ is the length of the shortest open path in the infinite open cluster between $x$ and $y$. For details, see [9].

We briefly sketch how the growth process approach provides an upper bound for $p_c(\mathbb{L}^3)$. Rotating $\mathbb{L}^3$ by a certain rotation matrix $R$ results in another embedding of the cubic lattice whose natural projection onto $\mathbb{R}^2$ is a triangular lattice (see Figure 1). Denote the rotated cubic lattice and its projection by $\mathbb{L}^3 \cdot R$ and $\mathbb{T}$, respectively. Let $\mathbf{0}^{(3)}$ denote the origin of $\mathbb{L}^3 \cdot R$ and $\mathbf{0}^{(2)}$ denote the origin of $\mathbb{T}$, which is the projection of $\mathbf{0}^{(3)}$.

https://doi.org/10.1017/jpr.2020.111 Published online by Cambridge University Press

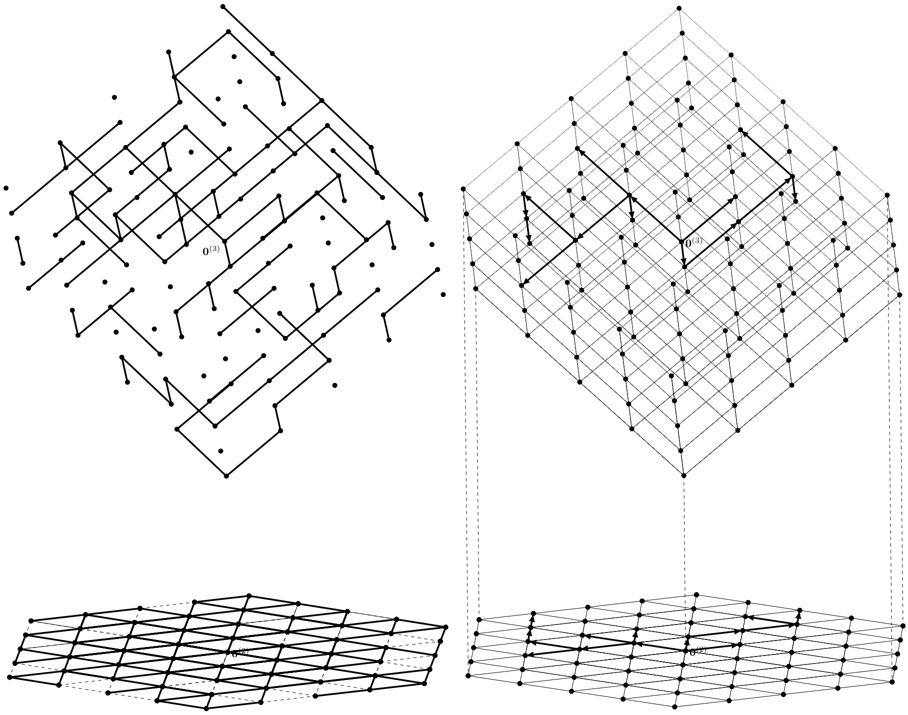


FIGURE 2. Upper left: A configuration $\omega^{(3)}$ on $\mathbb{L}^3 \cdot R$, with its open edges illustrated by thick line segments. Upper right: The three-dimensional growth process with $\omega^{(3)}$ as the underlying configuration. The arrows show how the edge cluster grows from the origin. Lower right: The projected growth process obtained from projection, forming a growth process on the triangular lattice. Lower left: The induced configuration on $\mathbb{T}$ obtained from the projected process. The open edges are marked by thick line segments. The two-dimensional open cluster is a subset of the projection of $C(\omega^{(3)})$.

Construct a three-dimensional growth process for each configuration $\omega^{(3)}$ on $\mathbb{L}^3 \cdot R$ as follows. Denote the open cluster containing $\mathbf{0}^{(3)}$ by $C(\omega^{(3)})$. We consider a growing edge cluster that contains open edges connecting $\mathbf{0}^{(3)}$ to vertices in $C(\omega^{(3)})$. The edge cluster is initialized as the empty set. At step 1, we explore from the origin $\mathbf{0}^{(3)}$ by considering the states ($\omega^{(3)}$-values) of its incident edges, and include its open incident edges in the edge cluster. Then, at each later step, we explore from a different vertex that is an endpoint of some edge in the edge cluster (see Figure 2) and expand the edge cluster by adding a subset of its open incident edges. Thus, we obtain a nondecreasing sequence of edge sets on $\mathbb{L}^3 \cdot R$ describing the growth of $C(\omega^{(3)})$ in terms of edges, which is called the three-dimensional growth process.

Projecting the three-dimensional growth process onto $\mathbb{R}^2$ yields a sequence of increasing edge sets on $\mathbb{T}$ (see Figure 2), which is called the projected growth process. At each step of the projected growth process, edges of $\mathbb{T}$ incident to a certain vertex are explored and a subset of the explored edges are included if they are projections of edges in the three-dimensional edge set. The included edges connect $\mathbf{0}^{(2)}$ to vertices in the projection of $C(\omega^{(3)})$.

The projected growth process can be related to a standard bond percolation process on $\mathbb{T}$ in the following manner. For each edge of $\mathbb{T}$ explored by the projected growth process at some step, we consider it to be open if and only if it is included by the process. The other edges of

https://doi.org/10.1017/jpr.2020.111 Published online by Cambridge University Press

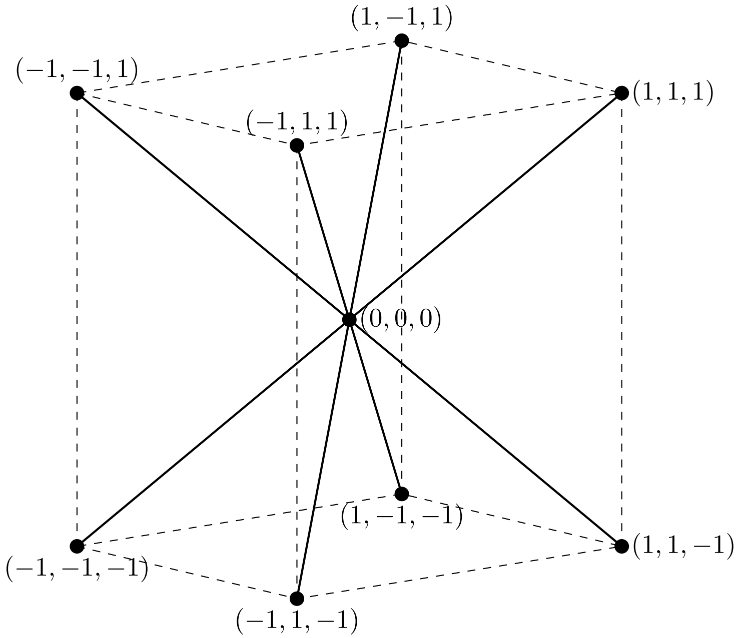


FIGURE 3. One cubic unit of the BCC lattice. Solid line segments represent edges of the BCC lattice, while dashed line segments form the boundary of the cubic unit, but are not edges of the BCC lattice.

$\mathbb{T}$ are designated to be open independently with probability $q$, where $q$ is the parameter of the (rotated) cubic lattice bond model. This provides us with a configuration on $\mathbb{T}$ (see Figure 2) whose distribution coincides with the probability measure of the bond percolation model on $\mathbb{T}$ with parameter $q$. We denote this configuration by $\omega^{(2)}$.

Let $C(\omega^{(2)})$ denote the open cluster containing $\mathbf{0}^{(2)}$ given the underlying configuration $\omega^{(2)}$ on $\mathbb{T}$. If $q > p_c(\mathbb{T}) = 2\sin\left(\frac{\pi}{18}\right)$, the probability that $C(\omega^{(2)})$ contains infinitely many vertices is strictly positive [36]. We show that $C(\omega^{(2)})$ is a subset of the endpoints of edges included in the projected growth process. Thus, the probability that the projected growth process, and furthermore the three-dimensional growth process, contain infinitely many edges is strictly positive. Consequently, we have $p_c(\mathbb{L}^3) = p_c(\mathbb{L}^3 \cdot R) \leqslant 2\sin\left(\frac{\pi}{18}\right) < 0.347\,297$. For comparison, recall that recent simulation results suggest $p_c(\mathbb{L}^3) \approx 0.2488$.

## 1.3. Application to the BCC lattice

We also consider another classic crystal structure known as the body-centered cubic (BCC) lattice, which we denote by $\mathbb{B}$. It is a vertex-transitive lattice with vertex degree eight. We embed $\mathbb{B}$ in $\mathbb{R}^3$ with vertices $(x,y,z)$ in $\mathbb{Z}^3$ for which $x = y = z \pmod 2$. Edges of $\mathbb{B}$ are between pairs of nearest-neighbor vertices, which are a Euclidean distance $\sqrt{3}$ apart. One may envision each vertex being located at the center of a cube with side length 2, with edges connected to each of the eight corners of the cube (see Figure 3). Denote the vertex and edge sets by $V^{\mathbb{B}}$ and $E^{\mathbb{B}}$, respectively.

As we did for the cubic lattice, we may construct a three-dimensional growth process on $\mathbb{B}$ and project it vertically onto $\mathbb{R}^2$ to form a projected growth process on a square lattice (which

https://doi.org/10.1017/jpr.2020.111 Published online by Cambridge University Press

has edges of length $\sqrt{2}$). By doing so, the three-dimensional growth process on $\mathbb{B}$ is related to a standard bond percolation process on the square lattice in such a way that one edge of the square lattice is open if and only if either of the two corresponding edges in $\mathbb{B}$ is open. Applying Kesten's [23] result that the percolation threshold of the square lattice is $\frac{1}{2}$, we obtain an upper bound.

**Theorem 2.** *For the bond percolation model,* $p_c(\mathbb{B}) \leqslant 1 - \sqrt{\frac{1}{2}}$.

The numerical upper bound obtained is 0.292 893, which may be compared to simulation results [26, 39] which suggest $p_c(\mathbb{B}) \approx 0.1802$.

### 1.4. Outline

The article is organized as follows. A coupling construction of the growth process approach for the cubic lattice is provided in Section 2. Related notation and definitions are listed in Section 2.1. Formal definitions of the three-dimensional growth process and its projection are provided in Section 2.2. Properties of the two processes are listed and proved in Section 2.3. The configuration $\omega^{(2)}$ is constructed in Section 2.4. The projected growth process is related to $C(\omega^{(2)})$ to provide an upper bound for $p_c(\mathbb{L}^3)$ in Section 2.5. Finally, we describe a direct application of the approach to the BCC lattice in Section 3, and comment on further generalizations and extensions of the approach in Section 4.

## 2. The growth process approach for the cubic lattice

### 2.1. Preliminaries and definitions

Consider the following rotation matrix on $\mathbb{R}^3$:

$$R =: \begin{bmatrix} \frac{1}{\sqrt{6}} & \frac{1}{\sqrt{2}} & \frac{1}{\sqrt{3}} \\ \frac{1}{\sqrt{6}} & -\frac{1}{\sqrt{2}} & \frac{1}{\sqrt{3}} \\ -\frac{2}{\sqrt{6}} & 0 & \frac{1}{\sqrt{3}} \end{bmatrix}.$$

The *rotated cubic lattice*, denoted by $\mathbb{L}^3 \cdot R = (\mathbb{Z}^3 \cdot R, \mathbb{E}^3 \cdot R)$, is an alternative embedding of the cubic lattice with $\mathbb{Z}^3 \cdot R = \{\mathbf{x} \cdot R \mid \mathbf{x} \in \mathbb{Z}^3\}$ and $\mathbb{E}^3 \cdot R = \{\{\mathbf{x} \cdot R, \mathbf{y} \cdot R\} \mid \{\mathbf{x}, \mathbf{y}\} \in \mathbb{E}^3\}$.

First, we introduce the following definitions for an infinite connected graph $G = (V, E)$ with vertex set $V$ and edge set $E$.

Let $\Omega := \{0, 1\}^E$ denote the *configuration space* of $G$, and $\mathcal{F}$ denote the $\sigma$-field generated by the finite cylinder sets of $\Omega$. Each $\omega = \{\omega(e) \mid e \in E\} \in \Omega$ is a *configuration* in which $\omega(e) = 1$ indicates that edge $e$ is open. Let $\mu_e(p)$ denote the Bernoulli measure on $\{0, 1\}$ with parameter $p$. Then $\mathbb{P}_p := \prod_{e \in E} \mu_e(p)$ is the *probability measure* for the bond percolation model on $G$ under which each edge is open independently with probability $p$. In particular, by taking $G$ as $\mathbb{L}^3 \cdot R$, the probability space is denoted by $(\Omega^{(3)}, \mathcal{F}^{(3)}, \mathbb{P}_p^{(3)})$; by taking $G$ as $\mathbb{T}$, the probability space is denoted by $(\Omega^{(2)}, \mathcal{F}^{(2)}, \mathbb{P}_p^{(2)})$.

Given a fixed vertex in $V$ called the origin and a configuration $\omega \in \Omega$, let $C(\omega) := \{u \in V \mid u$ is connected to the origin by $\omega$-open edges in $E\}$ be the *open cluster* containing the origin and $|C(\omega)|$ denote the number of vertices in $C(\omega)$. The *percolation probability* $\theta^G(p)$ is defined as $\theta^G(p) := \mathbb{P}_p(|C(\omega)| = \infty)$, and is nondecreasing with respect to $p$. The *bond percolation threshold* of $G$ is defined as $p_c(G) := sup\{p : \theta^G(p) = 0\}$.

https://doi.org/10.1017/jpr.2020.111 Published online by Cambridge University Press

Given $E_s \subset E$, the *endpoint set* of $E_s$, denoted by $\bigcup_{E_s}$, is the set of vertices in $V$ that are endpoints of at least one edge in $E_s$.

Given $V_s \subset V$, the *incident edge set* of $V_s$, denoted by $I[V_s]$, is the set of edges in $E$ incident to at least one vertex in $V_s$.

Now we specialize to the lattices $\mathbb{L}^3{\cdot}R$ and $\mathbb{T}$. For each $\mathbf{x} = (x_1, x_2, x_3) \in \mathbb{Z}^3{\cdot}R$, the *projection* of $\mathbf{x}$ is $proj(\mathbf{x}) := (x_1, x_2)$. Naturally, for each $\{\mathbf{x}, \mathbf{y}\} \in \mathbb{E}^3{\cdot}R$, its projection is $proj(\{\mathbf{x}, \mathbf{y}\}) := \{proj(\mathbf{x}), proj(\mathbf{y})\}$. More generally, given $V_s \subseteq \mathbb{Z}^3{\cdot}R$ and $E_s \subseteq \mathbb{E}^3{\cdot}R$, the corresponding projections are $proj(V_s) := \{proj(v) \mid v \in V_s\}$ and $proj(E_s) := \{proj(e) \mid e \in E_s\}$, respectively.

Let $\mathbb{T} = (V^{\mathbb{T}}, E^{\mathbb{T}})$ be an embedding of the *triangular lattice* in $\mathbb{R}^2$, where

$$V^{\mathbb{T}} = proj(\mathbb{Z}^3{\cdot}R) = \left\{ k_1\left(\frac{1}{\sqrt{6}}, \frac{1}{\sqrt{2}}\right) + k_2\left(\frac{2}{\sqrt{6}}, 0\right) \middle| k_1, k_2 \in \mathbb{Z} \right\}$$

and

$$E^{\mathbb{T}} = proj(\mathbb{E}^3{\cdot}R) = \left\{ \{\mathbf{x}, \mathbf{y}\} \middle| \mathbf{x}, \mathbf{y} \in V^{\mathbb{T}}, \ \|\mathbf{x} - \mathbf{y}\| = \frac{2}{\sqrt{6}} \right\}.$$

For each $\mathbf{x} \in V^{\mathbb{T}}$, we define its *associated column* as $col(\mathbf{x}) := \{\mathbf{y} \in \mathbb{Z}^3{\cdot}R \mid proj(\mathbf{y}) = \mathbf{x}\}$. More generally, for each $V_s \subseteq \mathbb{T}$, its *associated columns* are $col(V_s) := \bigcup_{\mathbf{x} \in V_s} col(\mathbf{x})$. Accordingly, for each $\mathbf{x} \in \mathbb{Z}^3{\cdot}R$ or $V_s \subseteq \mathbb{Z}^3{\cdot}R$, its *associated column* is defined as the associated column of its projection.

Fix a deterministic ordering of $V^{\mathbb{T}}$ by assigning each vertex $v$ a distinct positive integer $l(v)$. Extend the domain of $l$ to $\mathbb{Z}^3{\cdot}R$ by defining $l(v) = l(proj(v))$ for all $v \in \mathbb{Z}^3{\cdot}R$. For any vertex, $l(v)$ is called the *label* of $v$.

### 2.2. The growth process and its projection

We now provide a formal recursive definition of the growth process, introduce notation, and briefly interpret aspects of the definition.

**Definition 1.** (*The growth process* $\mathbf{G}^{(3)}$.) Initialize $\left(A_0^{(3)}, C_0^{(3)}, D_0^{(3)}\right)$ as $(\emptyset, \{\mathbf{0}^{(3)}\}, \emptyset)$. Given a labeling function $l$, define a stochastic process $\left(v_n^{(3)}, A_n^{(3)}, B_n^{(3)}, C_n^{(3)}, D_n^{(3)}\right):\Omega^{(3)} \to \mathbb{Z}^3{\cdot}R \times 2^{\mathbb{Z}^3\cdot R} \times 2^{\mathbb{E}^3\cdot R} \times 2^{\mathbb{Z}^3\cdot R} \times 2^{\mathbb{E}^3\cdot R}$ on $\left(\Omega^{(3)}, \mathcal{F}^{(3)}, \mathbb{P}_q^{(3)}\right)$ for all $n \geqslant 1$ recursively as follows. For each $\omega^{(3)} \in \Omega^{(3)}$, assume that the process has been defined up to step $n$. At step $n+1$, if $C_n^{(3)} \setminus A_n^{(3)} \neq \emptyset$, define

$$\begin{aligned}
v_{n+1}^{(3)} &:= \arg\min \left\{ l(v) : v \in C_n^{(3)} \setminus A_n^{(3)} \right\}, \\
A_{n+1}^{(3)} &:= A_n^{(3)} \cup \left\{ v_{n+1}^{(3)} \right\}, \\
B_{n+1}^{(3)} &:= I\left[\left\{ v_{n+1}^{(3)} \right\}\right] \setminus I\left[ col\left( C_n^{(3)} \setminus \left\{ v_{n+1}^{(3)} \right\} \right) \right], \\
D_{n+1}^{(3)} &:= D_n^{(3)} \cup \{ e \in B_{n+1}^{(3)} : \omega^{(3)}(e) = 1 \}, \\
C_{n+1}^{(3)} &:= C_n^{(3)} \cup \left( \bigcup_{D_{n+1}^{(3)}} \right).
\end{aligned}$$

Otherwise, we define $\left(v_{n+1}^{(3)}, A_{n+1}^{(3)}, B_{n+1}^{(3)}, C_{n+1}^{(3)}, D_{n+1}^{(3)}\right) := \left(v_n^{(3)}, A_n^{(3)}, \emptyset, C_n^{(3)}, D_n^{(3)}\right)$.

The *growth process associated with* $\omega^{(3)}$ is the stochastic process $\mathbf{G}_n^{(3)} := \left(A_n^{(3)}, D_n^{(3)}\right)$ defined on the probability space $\left(\Omega^{(3)}, \mathcal{F}^{(3)}, \mathbb{P}_q^{(3)}\right)$.

https://doi.org/10.1017/jpr.2020.111 Published online by Cambridge University Press

To aid in interpreting the definition, we provide the following terminology and explanation. Consider a fixed configuration $\omega^{(3)} \in \Omega^{(3)}$. To *explore* from a vertex means to determine which edges incident to the vertex are open. At step $n$ of the growth process, we call $C_n^{(3)}$ the *vertex cluster*, $D_n^{(3)}$ the *edge cluster*, and $A_n^{(3)}$ the *antecedent set*. The antecedent set $A_n^{(3)}$ is the set of vertices from which the process has already explored, and from which future exploration is prohibited. From the vertices in the vertex cluster which are not in the antecedent set, choose $v_{n+1}^{(3)}$ to be the vertex with the smallest label. (As we shall see in Lemma 1, there is a unique such vertex.) From $v_{n+1}^{(3)}$, identify its incident edges which are not incident to any vertex sharing the same projection as a vertex in $C_n^{(3)} \setminus \{v_{n+1}^{(3)}\}$. We call this set the *exploration region* $B_{n+1}^{(3)}$ for step $(n+1)$. After exploring the edges in $B_{n+1}^{(3)}$ from $v_{n+1}^{(3)}$, the open edges are included in the edge cluster $D_{n+1}^{(3)}$ and their endpoints are included in the vertex cluster $C_{n+1}^{(3)}$. By induction, the construction of the exploration regions insures that at most one vertex in any column of $\mathbb{Z}^3$, and that at most one edge in any column, is explored. Thus, $v_n^{(3)}$ is unique for each $n$, being from the column with the smallest label. Finally, the vertex $v_{n+1}^{(3)}$ is added to the antecedent set $A_n^{(3)}$ to produce $A_{n+1}^{(3)}$ to insure the exploration from it does not occur again.

Projecting $\mathbf{G}^{(3)}$ onto $\mathbb{R}^2$ results in the projected growth process, which is denoted by $\mathbf{G}^{(2)}$.

**Definition 2.** (*The projected growth process* $\mathbf{G}^{(2)}$) Let $\left(v_n^{(2)}, A_n^{(2)}, B_n^{(2)}, C_n^{(2)}, D_n^{(2)}\right) \in V^{\mathbb{T}} \times 2^{V^{\mathbb{T}}} \times 2^{E^{\mathbb{T}}} \times 2^{V^{\mathbb{T}}} \times 2^{E^{\mathbb{T}}}$ be a stochastic process on $\left(\Omega^{(3)}, \mathcal{F}^{(3)}, \mathbb{P}_q^{(3)}\right)$, where $v_n^{(2)} := proj\left(v_n^{(3)}\right)$, $A_n^{(2)} := proj\left(A_n^{(3)}\right), \ldots$, and $D_n^{(2)} := proj\left(D_n^{(3)}\right)$. Define the *projected growth process associated with* $\omega^{(3)}$ as $\mathbf{G}_n^{(2)} := \left(A_n^{(2)}, D_n^{(2)}\right)$.

In $\mathbf{G}^{(2)}$ and $\mathbf{G}^{(3)}$, the edge clusters $D_n^{(2)}$ and $D_n^{(3)}$ are both nondecreasing in $n$. For simplicity, denote $\bigcup_{n=1}^{\infty} D_n^{(2)}$ and $\bigcup_{n=1}^{\infty} D_n^{(3)}$ by $D_\infty^{(2)}$ and $D_\infty^{(3)}$, respectively.

### 2.3. Properties of $\mathbf{G}^{(3)}$ and $\mathbf{G}^{(2)}$

We observe the following properties regarding the growth process $\mathbf{G}^{(3)}$.

**Lemma 1.** *For each pair of distinct edges* $e_1, e_2 \in D_\infty^{(3)}$, $proj(e_1) \neq proj(e_2)$.

Lemma 1 follows from the construction of exploration regions: $B_{n+1}^{(3)}$ excludes all edges incident to vertices in $col(C_n^{(3)} \setminus \{v_{n+1}^{(3)}\})$, thus does not contain edges having the same projection with edges in $D_n^{(3)}$. That is, $proj(B_{n+1}^{(3)}) \bigcap proj(D_n^{(3)}) = \emptyset$ for each $n \in \mathbb{N}$. By induction on $n$, we have that any two edges in $D_\infty^{(3)}$ have distinct projections.

Lemma 1 implies that the natural projection defines a bijection from $D_\infty^{(3)}$ to $D_\infty^{(2)}$. Moreover, it defines a bijection from $D_n^{(3)} \setminus D_{n-1}^{(3)}$ to $D_n^{(2)} \setminus D_{n-1}^{(2)}$ for each $n \in \mathbb{N}_+$. This property makes it easier to analyze the distribution of $\mathbf{G}^{(2)}$.

**Lemma 2.** *For each* $\omega^{(3)} \in \Omega^{(3)}$ *and* $n \in \mathbb{N}$, *we have*

$$C_n^{(3)}\left(\omega^{(3)}\right) \subseteq C\left(\omega^{(3)}\right). \tag{1}$$

Lemma 2 states that at step $n$ of the growth process $\mathbf{G}^{(3)}\left(\omega^{(3)}\right)$, its vertex cluster is a subset of the open cluster of the underlying configuration $\omega^{(3)}$, which can be proved easily by induction on $n$.

https://doi.org/10.1017/jpr.2020.111 Published online by Cambridge University Press

**Lemma 3.** *The conditional joint distribution of* $D_n^{(3)} \setminus D_{n-1}^{(3)}$ *given* $B_n^{(3)}$ *is*

$$\mathbb{P}_q^{(3)}\left(D_n^{(3)} \setminus D_{n-1}^{(3)} \mid B_n^{(3)}\right) = q^{|D_n^{(3)} \setminus D_{n-1}^{(3)}|}(1-q)^{|B_n^{(3)}|-|D_n^{(3)} \setminus D_{n-1}^{(3)}|},$$

*where* $|\cdot|$ *represents the cardinality of the underlying set.*

From Definition 1, each edge $e \in B_n^{(3)}$ is added to $D_n^{(3)} \setminus D_{n-1}^{(3)}$ if and only if $\omega^{(3)}(e) = 1$, where $\{\omega^{(3)}(e): e \in B_n^{(3)}\}$ follow independent Bernoulli distributions with parameter $q$ given $B_n^{(3)}$. Thus, Lemma 3 follows.

Naturally, the process $\mathbf{G}^{(2)}$, which is the projection of $\mathbf{G}^{(3)}$, also has these properties.

**Lemma 4.** *For each* $\omega^{(3)} \in \Omega^{(3)}$ *and* $n \in \mathbb{N}$, $C_n^{(2)}(\omega^{(3)}) \subseteq proj(C(\omega^{(3)}))$.

Lemma 4 is a direct consequence of Lemma 2, where we simply perform projection on both sides of (1).

**Lemma 5.** *The conditional joint distribution of* $D_n^{(2)} \setminus D_{n-1}^{(2)}$ *given* $B_n^{(2)}$ *is*

$$\mathbb{P}_q^{(3)}\left(D_n^{(2)} \setminus D_{n-1}^{(2)} \mid B_n^{(2)}\right) = q^{|D_n^{(2)} \setminus D_{n-1}^{(2)}|}(1-q)^{|B_n^{(2)}|-|D_n^{(2)} \setminus D_{n-1}^{(2)}|}. \tag{2}$$

Intuitively, Lemma 5 is a direct result of Lemmas 1 and 3: For each edge $e \in B_n^{(2)}$, $e$ is added to $D_n^{(2)} \setminus D_{n-1}^{(2)}$ if and only if the unique edge in $B_n^{(3)}$ whose projection is $e$ is open. Mathematically, we may condition on $B_n^{(3)}$ and utilize the law of total probability: Given $B_n^{(2)}$, there are countably infinitely many possibilities for $B_n^{(3)}$ such that $proj\left(B_n^{(3)}\right) = B_n^{(2)}$. Meanwhile, each edge $e \in B_n^{(2)}$ is added to $D_n^{(2)} \setminus D_{n-1}^{(2)}$ if and only if the unique edge in $B_n^{(3)}$ whose projection is $e$ is added to $D_n^{(3)} \setminus D_{n-1}^{(3)}$. Thus, by Lemmas 1 and 3, we have

$$\begin{aligned}
\mathbb{P}_q^{(3)}\left(D_n^{(2)} \setminus D_{n-1}^{(2)} \mid B_n^{(2)}\right) &= \sum_{B_n^{(3)}} \mathbb{P}_q^{(3)}\left(D_n^{(3)} \setminus D_{n-1}^{(3)} \mid B_n^{(3)}\right) \cdot \mathbb{P}_q^{(3)}\left(B_n^{(3)} \mid B_n^{(2)}\right) \\
&= \sum_{B_n^{(3)}} q^{|D_n^{(3)} \setminus D_{n-1}^{(3)}|} \cdot (1-q)^{|B_n^{(3)}|-|D_n^{(3)} \setminus D_{n-1}^{(3)}|} \cdot \mathbb{P}_q^{(3)}\left(B_n^{(3)} \mid B_n^{(2)}\right) \\
&= \sum_{B_n^{(3)}} q^{|D_n^{(2)} \setminus D_{n-1}^{(2)}|} \cdot (1-q)^{|B_n^{(2)}|-|D_n^{(2)} \setminus D_{n-1}^{(2)}|} \cdot \mathbb{P}_q^{(3)}\left(B_n^{(3)} \mid B_n^{(2)}\right) \\
&= q^{|D_n^{(2)} \setminus D_{n-1}^{(2)}|} \cdot (1-q)^{|B_n^{(2)}|-|D_n^{(2)} \setminus D_{n-1}^{(2)}|},
\end{aligned}$$

where the summations are taken over all $B_n^{(3)} \subseteq \mathbb{E}^3 \cdot R$ such that $proj\left(B_n^{(3)}\right) = B_n^{(2)}$.

We end this subsection with another observation regarding the projected growth process $\mathbf{G}_n^{(2)}$.

**Lemma 6.** *For each* $\omega^{(3)} \in \Omega^{(3)}$, *the sets* $\left\{B_n^{(2)}\left(\omega^{(3)}\right)\right\}_{n=1}^{\infty}$ *are pairwise disjoint.*

Lemma 6 follows from the construction of $\left\{B_n^{(3)}\right\}$ in Definition 1, and we shall use it to prove Lemma 7 in the following subsection.

https://doi.org/10.1017/jpr.2020.111 Published online by Cambridge University Press

### 2.4. The induced configuration

Using the projected growth process, we construct a configuration on $\mathbb{T}$ as follows.

**Definition 3.** For each $\big(\omega^{(3)}, \tilde{\omega}^{(2)}\big) \in \Omega^{(3)} \times \Omega^{(2)}$, let $\mathbf{G}^{(2)}$ be the projected growth process associated with $\omega^{(3)}$. The induced configuration is a configuration in $\Omega^{(2)}$ such that, for each $e \in V^{\mathbb{T}}$,

$$\omega^{(2)}(e) := \begin{cases} 1 & \text{if } e \in D_\infty^{(2)}, \\ 0 & \text{if } e \in \big(\bigcup_{n=1}^\infty B_n^{(2)}\big) \setminus D_\infty^{(2)}, \\ \tilde{\omega}^{(2)}(e) & \text{otherwise.} \end{cases} \tag{3}$$

In Definition 3 the configuration $\tilde{\omega}^{(2)}$ is introduced to determine the states of the edges of $\mathbb{T}$ that are not explored by the projected process $\mathbf{G}^{(2)}$. For the induced configuration $\omega^{(2)}$, we have the following result.

**Lemma 7.** *If* $\big(\omega^{(3)}, \tilde{\omega}^{(2)}\big) \in \Omega^{(3)} \times \Omega^{(2)}$ *is* $\mathbb{P}_q$ *distributed, where* $\mathbb{P}_q := \mathbb{P}_q^{(3)} \times \mathbb{P}_q^{(2)}$, *then the induced configuration* $\omega^{(2)}$ *is* $\mathbb{P}_q^{(2)}$ *distributed.*

Lemma 7 is intuitively straightforward. For each $e \in \bigcup_{n=1}^\infty B_n^{(2)}$, by Lemma 6 there exists a unique $i \in \mathbb{N}$ such that $e \in B_i^{(2)}$. Thus, $\omega^{(2)}(e) = 1$ if and only if $e \in D_i^{(2)}$, which implies that $\omega^{(2)}(e)$ is Bernoulli distributed with parameter $q$ by Lemma 5. Meanwhile, for each $e \notin \bigcup_{n=1}^\infty B_n^{(2)}$, we have $\omega^{(2)}(e) = \tilde{\omega}^{(2)}(e)$ also being Bernoulli distributed with parameter $q$. Consequently, $\omega^{(2)}(e)$ is Bernoulli distributed with parameter $q$, regardless of whether $e$ is in $\bigcup_{n=1}^\infty B_n^{(2)}$ or not. Notice that $\omega^{(2)}(e)$ depends on the $\omega^{(3)}$- or $\tilde{\omega}^{(2)}$-values of distinct edges in either $\mathbb{E}^3 \cdot R$ or $E^{\mathbb{T}}$ for each $e \in E^{\mathbb{T}}$, and $\{\omega^{(3)}(e)\}_{e \in \mathbb{E}^3 \cdot R}$ and $\{\tilde{\omega}^{(2)}(e)\}_{e \in E^{\mathbb{T}}}$ are mutually independent. Consequently, $\{\omega^{(2)}(e)\}_{e \in E^{\mathbb{T}}}$ are independent.

Although it may seem intuitive, a comprehensive proof of Lemma 7 is somewhat long and is provided in the Appendix.

Another property of the induced configuration $\omega^{(2)}$ is that $C(\omega^{(2)})$ is a subset of the projected vertex cluster.

**Lemma 8.** *For each* $\big(\omega^{(3)}, \tilde{\omega}^{(2)}\big) \in \Omega^{(3)} \times \Omega^{(2)}$, *let* $\omega^{(2)}$ *be the induced configuration and* $\mathbf{G}^{(2)}$ *be the projected growth process associated with* $\omega^{(3)}$. *Then* $C(\omega^{(2)}) \subseteq \bigcup_{D_\infty^{(2)}}$.

*Proof.* For each $v \in C(\omega^{(2)})$, by the definition of an open cluster there exists an open path $\{w_0 = \mathbf{0}^{(2)}, w_1, w_2, \ldots, w_k = v\}$ of some length $k$ that connects $v$ to $\mathbf{0}^{(2)}$, i.e. $\omega^{(2)}(\{w_i, w_{i+1}\}) = 1$ for all $i \in \{0, 1, \ldots, k-1\}$. We prove that $w_i \in \bigcup_{D_\infty^{(2)}}$ for all $i \in \{0, 1, \ldots, k\}$ by applying induction on $i$.

For $i = 1$ we have $\{w_0, w_1\} \in B_1^{(2)}$. Since $\omega^{(2)}(\{w_0, w_1\}) = 1$, according to (3) we obtain $1 = \omega^{(2)}(\{w_0, w_1\}) = \mathbf{1}_{\{\{w_0, w_1\} \in D_\infty^{(2)}\}}$. Consequently, $w_1 \in \bigcup_{D_\infty^{(2)}}$.

Assume that $w_0, w_1, \ldots, w_i \in \bigcup_{D_\infty^{(2)}}$. We need to show that $w_{i+1} \in \bigcup_{D_\infty^{(2)}}$ as well. By the induction hypothesis, $w_i \in \bigcup_{D_\infty^{(2)}}$. Thus, there exists $j \in \mathbb{N}$ such that $v_j^{(2)} = w_i$. Consider the following two cases.

Case 1: If $\{w_i, w_{i+1}\} \in B_j^{(2)}$, then $\mathbf{1}_{\{\{w_i, w_{i+1}\} \in D_\infty^{(2)}\}} = \omega^{(2)}(\{w_i, w_{i+1}\}) = 1$. Consequently, $w_{i+1} \in \bigcup_{D_\infty^{(2)}}$.

Case 2: If $\{w_i, w_{i+1}\} \notin B_j^{(2)}$, then $w_{i+1}$ has been included in the vertex cluster $C^{(2)}$ before step $j$ of $\mathbf{G}^{(2)}$. More specifically, since $B_j^{(2)} = proj\big(B_j^{(3)}\big) = I\big[\big\{v_j^{(2)}\big\}\big] \setminus I\big[\bigcup_{D_{j-1}^{(2)}} \setminus \big\{v_j^{(2)}\big\}\big]$,

https://doi.org/10.1017/jpr.2020.111 Published online by Cambridge University Press

we have $\{w_i, w_{i+1}\} = \{v_j^{(2)}, w_{i+1}\} \notin B_j^{(2)}$ if and only if $w_{i+1} \in \bigcup_{D_{j-1}^{(2)}}$. Consequently, $w_{i+1} \in \bigcup_{D_\infty^{(2)}}$.

In summary, $w_{i+1} \in \bigcup_{D_\infty^{(2)}}$. Using induction, we conclude that $v \in \bigcup_{D_\infty^{(2)}}$. Since $v$ is an arbitrary vertex in $C(\omega^{(2)})$, we have $C(\omega^{(2)}) \subseteq \bigcup_{D_\infty^{(2)}}$.

### 2.5. An upper bound for $p_c(\mathbb{L}^3)$

Now we are ready to prove Theorem 1.

*Proof.* Since, under $\mathbb{P}_q$ measure, the marginal distribution of $\omega^{(3)}$ is $\mathbb{P}_q^{(3)}$,

$$\mathbb{P}_q^{(3)}\big(|C(\omega^{(3)})| = \infty\big) = \mathbb{P}_q\big(|C(\omega^{(3)})| = \infty\big). \tag{4}$$

By Lemma 2,

$$\mathbb{P}_q\big(|C(\omega^{(3)})| = \infty\big) \geqslant \mathbb{P}_q\left(\left|\bigcup_{n=1}^{\infty} C_n^{(3)}(\omega^{(3)})\right| = \infty\right). \tag{5}$$

From Definitions 1 and 2,

$$\begin{aligned}\mathbb{P}_q\left(\left|\bigcup_{n=1}^{\infty} C_n^{(3)}(\omega^{(3)})\right| = \infty\right) &= \mathbb{P}_q\left(\left|\bigcup_{D_\infty^{(3)}(\omega^{(3)})}\right| = \infty\right)\\ &= \mathbb{P}_q\left(\left|\bigcup_{D_\infty^{(2)}(\omega^{(3)})}\right| = \infty\right).\end{aligned} \tag{6}$$

Using Lemma 8,

$$\mathbb{P}_q\left(\left|\bigcup_{D_\infty^{(2)}(\omega^{(3)})}\right| = \infty\right) \geqslant \mathbb{P}_q(|C(\omega^{(2)})| = \infty). \tag{7}$$

Also, in Lemma 7 we proved that $\omega^{(2)}$ is $\mathbb{P}_q^{(2)}$ distributed. Thus,

$$\mathbb{P}_q(|C(\omega^{(2)})| = \infty) = \mathbb{P}_q^{(2)}(|C(\omega^{(2)})| = \infty) > 0 \tag{8}$$

for all $q > p_c(\mathbb{T})$. This proves that $\mathbb{P}_q^{(3)}(|C(\omega^{(3)})| = \infty) > 0$ for all $q > p_c(\mathbb{T})$ by (4)–(8). Consequently, $p_c(\mathbb{L}^3) = p_c(\mathbb{L}^3 \cdot R) \leqslant p_c(\mathbb{T})$.

## 3. Application to the BCC lattice

Given the embedding of $\mathbb{B}$ described in Section 1.3, performing the natural projection of $\mathbb{B}$ results in a square lattice with edges of length $\sqrt{2}$. Denote this lattice by $\sqrt{2}\mathbb{L}^2$, with vertex set $\mathbb{V}$ and edge set $\mathbb{E}$.

The definitions of natural projection and associated column for $\mathbb{L}^3 \cdot R$ and $\mathbb{T}$ can be generalized to lattices $\mathbb{B}$ and $\sqrt{2}\mathbb{L}^2$ in a straightforward manner. Meanwhile, a labeling function is defined for vertices in $\sqrt{2}\mathbb{L}^2$ and extended to vertices in $\mathbb{B}$. For simplicity, we shall abuse notation by using the same notation as introduced in the previous section.

### 3.1. The BCC growth process and its projection

The growth process for $\mathbb{B}$ can be defined following a similar procedure to defining the growth process for $\mathbb{L}^3 \cdot R$. For simplicity we denote the growth process for $\mathbb{B}$ by $\mathbf{G}^{(3)}$ as well, and all the other notation carries over analogously. For each configuration $\omega^{(3)}$ of $\mathbb{B}$, the growth process associated with $\omega^{(3)}$ is defined recursively as follows.

https://doi.org/10.1017/jpr.2020.111 Published online by Cambridge University Press

Initialize $A_0^{(3)} = \emptyset$, $C_0^{(3)} = \{\mathbf{0}^{(3)}\}$, and $D_0^{(3)} = \emptyset$, where $\mathbf{0}^{(3)}$ denotes the origin of $\mathbb{B}$ throughout this section. Let $l$ be a labeling function on $\mathbb{V}$ and extend its domain to $V^{\mathbb{B}}$ in the same way as before. Assume that the processes are defined up to step $n$. At step $n+1$, if $C_n^{(3)} \setminus A_n^{(3)} \neq \emptyset$, then $v_{n+1}^{(3)} := \arg\min \{l(v): v \in C_n^{(3)} \setminus A_n^{(3)}\}$, $A_{n+1}^{(3)} := A_n^{(3)} \cup \{v_{n+1}^{(3)}\}$, and $B_{n+1}^{(3)} := I\big[\{v_{n+1}^{(3)}\}\big] \setminus I\big[col\big(C_n^{(3)} \setminus \{v_{n+1}^{(3)}\}\big)\big]$, all of which are defined in the same manner as in Definition 1. Meanwhile, the edge cluster is updated in a slightly different manner: a subset of open edges is included in $D_{n+1}^{(3)}$ such that no two edges in $D_{n+1}^{(3)}$ share the same projection. That is, $D_{n+1}^{(3)} := D_n^{(3)} \cup \big\{\{\mathbf{x}, v_{n+1}^{(3)}\} \in B_{n+1}^{(3)} \mid \omega^{(3)}\big(\{\mathbf{x}, v_{n+1}^{(3)}\}\big) = 1$, there does not exist $\{\mathbf{x}', v_{n+1}^{(3)}\} \in B_{n+1}^{(3)}$ such that $proj(\mathbf{x}') = proj(\mathbf{x})$, $\omega^{(3)}\big(\{\mathbf{x}', v_{n+1}^{(3)}\}\big) = 1$, and $x_3{}' < x_3\big\}$. Subsequently, the vertex cluster is updated by $C_{n+1}^{(3)} = C_n^{(3)} \cup \big(\bigcup_{D_{n+1}^{(3)}}\big)$.

Following Definition 2, the projected growth process can be defined analogously for the BCC lattice. Denote the process by $\mathbf{G}^{(2)}$; its associated notation is defined in terms of the projection of the corresponding three-dimensional notation as in Definition 2. Notice that at step $n$ of $\mathbf{G}^{(2)}$, each edge $e$ in $B_n^{(2)}$ is added to $D_n^{(2)}$ if and only if either of the two edges in $B_n^{(3)}$ whose projections are $e$ is open. (If both edges are open, the 'lower' edge is included in the three-dimensional edge cluster, as specified in the definition of $D_n^{(3)}$ above.) Thus, the conditional probability, given $e \in B_n^{(2)}$, of $e$ being added to $D_n^{(2)}$ is $2q - q^2$. This gives us the following fact.

**Fact 1.** *Let $\mathbb{P}_q^{(3)}$ be the probability measure for the bond percolation model on $\mathbb{B}$ with parameter $q$, and $\mathbf{G}^{(2)}$ be its projected growth process. The conditional joint distribution of $D_n^{(2)} \setminus D_{n-1}^{(2)}$ given $B_n^{(2)}$ is*

$$\mathbb{P}_q^{(3)}\big(D_n^{(2)} \setminus D_{n-1}^{(2)} \mid B_n^{(2)}\big) = (2q - q^2)^{|D_n^{(2)} \setminus D_{n-1}^{(2)}|}(1 - 2q + q^2)^{|B_n^{(2)}| - |D_n^{(2)} \setminus D_{n-1}^{(2)}|}.$$

### 3.2. The induced configuration $\omega^{(2)}$

We construct an induced configuration $\omega^{(2)}$ on $\sqrt{2}\mathbb{L}^2$ using the projected growth process $\mathbf{G}^{(2)}$: for each edge $e \in \bigcup_{n=1}^{\infty} B_n^{(2)}$, let $\omega^{(2)}(e) = 1$ if and only if $e \in D_\infty^{(2)}$; for each edge $e \notin \bigcup_{n=1}^{\infty} B_n^{(2)}$, let $\omega^{(2)}(e) = 1$ with probability $2q - q^2$, independent of the $\omega^{(3)}$- and $\omega^{(2)}$-values of all the other edges in $\mathbb{E}$.

The induced configuration $\omega^{(2)}$ inherits the two properties of the induced configuration defined for the square lattice.

**Fact 2.** *Each edge of $\mathbb{E}$ is $\omega^{(2)}$-open with probability $2q - q^2$, independently of all the other edges.*

**Fact 3.** *The open cluster $C(\omega^{(2)})$ is a subset of the projected vertex cluster, i.e. $C(\omega^{(2)}) \subseteq \bigcup_{D_\infty^{(2)}}$.*

### 3.3. An upper bound for $p_c(\mathbb{B})$

Follow the reasoning in the proof of Theorem 1. When $q$ is chosen such that $2q - q^2 > p_c(\mathbb{L}^2) = \frac{1}{2}$, the probability that $|C(\omega^{(2)})|$ is infinite is strictly positive by Fact 2, which further implies that $\big|\bigcup_{D_\infty^{(2)}}\big|$ is infinite with strictly positive probability. Therefore, the probability that $|C(\omega^{(3)})| = \infty$ is strictly positive as well, making $q$ an upper bound for $p_c(\mathbb{B})$. Solving for the infimum of $q$ satisfying $2q - q^2 > \frac{1}{2}$, we obtain Theorem 2.

https://doi.org/10.1017/jpr.2020.111 Published online by Cambridge University Press

## 4. Further discussion

This article shows two simple applications of the growth process approach. In the projected growth process defined for either of the two applications, edges of the two-dimensional lattice are added to the cluster following independent Bernoulli measures (see (2)). Subsequently, the induced configuration can be constructed in a straightforward manner. However, to describe the expansion of the open cluster on some other three-dimensional lattices, a more complicated three-dimensional growth process has to be defined. Thus, the probability measure of the corresponding projected growth process is not characterizable by independent Bernoulli measures, and the induced configuration has to be constructed in a different way. In [52] there is an extension of the growth process approach to stacked lattices by dealing with the complication of defining the induced configuration by means of replication and coupling. This generalized approach can be further applied to the BCC lattice, which provides an even smaller upper bound for $p_c(\mathbb{B})$. Also, see [52] for another extension of the growth process approach, applied to the third common crystal lattice structure, the face-centered cubic lattice. The growth process definition is considerably more complicated, the projected process is compared to a multi-parameter model, and graph-welding and network flow techniques must be used to determine the upper bound.

## Appendix A. Formal proof of Lemma 7

*Proof.* For each $E \subset E^{\mathbb{T}}$, $|E| < \infty$, define $C_+(E) := \{\omega \in \Omega^{(2)} \mid \omega(e) = 1 \text{ for all } e \in E\} \subset \Omega^{(2)}$ to be its corresponding *positive cylinder set*. Notice that $C_+(E_1) \cap C_+(E_2) = C_+(E_1 \cap E_2)$ for all $E_1, E_2 \subseteq E^{\mathbb{T}}$, i.e. the positive cylinder sets form a $\pi$-system. Notice also that $\mathcal{F}^{(2)} = \sigma(\{C_+(E) \mid E \subset E^{\mathbb{T}},\ |E| < \infty\})$. By the $\pi$–$\lambda$ theorem, in order to show that $\omega^{(2)}$ is $\mathbb{P}_q^{(2)}$ distributed, we only need to show that

$$\mathbb{P}_q(\omega^{(2)} \in C_+(E)) = \mathbb{P}_q^{(2)}(C_+(E)) = q^{|E|} \tag{9}$$

for each $E \subset E^{\mathbb{T}}$ and $|E| < \infty$. We prove (9) by induction on $|E|$.

For the base case where $|E| = 1$, let $E = \{e\}$ be the set of edges of interest. Furthermore, let $\mathbf{1}(e)$ be the (random) indicator that there exists $n \in \mathbb{N}$ such that $e \in B_n^{(2)}$. By (2) and (3),

$$\begin{aligned}
&\mathbb{P}_q(\omega^{(2)}(e) = 1 \mid \mathbf{1}(e) = 1) \\
&\qquad = \sum_{n=1}^{\infty} \mathbb{P}_q\big(\omega^{(2)}(e) = 1 \mid e \in B_n^{(2)}, \mathbf{1}(e) = 1\big) \cdot \mathbb{P}_q\big(e \in B_n^{(2)} \mid \mathbf{1}(e) = 1\big) \\
&\qquad = \sum_{n=1}^{\infty} \sum_{v \in V^{\mathbb{T}}} \sum_{B \subseteq I[\{v\}]} \mathbb{P}_q\big(\omega^{(2)}(e) = 1 \mid e \in B_n^{(2)}, B_n^{(2)} = B\big) \\
&\qquad\qquad \cdot \mathbb{P}_q\big(e \in B_n^{(2)}, B_n^{(2)} = B \mid \mathbf{1}(e) = 1\big) \\
&\qquad = q \cdot \sum_{n=1}^{\infty} \sum_{v \in V^{\mathbb{T}}} \sum_{B \subseteq I[\{v\}]} \mathbb{P}_q\big(e \in B_n^{(2)}, B_n^{(2)} = B \mid \mathbf{1}(e) = 1\big) \\
&\qquad = q.
\end{aligned}$$

https://doi.org/10.1017/jpr.2020.111 Published online by Cambridge University Press

Thus,

$$\begin{aligned}
&\mathbb{P}_q\big(\omega^{(2)} \in C_+(E)\big) \\
&= \mathbb{P}_q\big(\omega^{(2)}(e) = 1 \mid \mathbf{1}(e) = 1\big) \cdot \mathbb{P}_q(\mathbf{1}(e) = 1) + \mathbb{P}_q\big(\omega^{(2)}(e) = 1 \mid \mathbf{1}(e) = 0\big) \cdot \mathbb{P}_q(\mathbf{1}(e) = 0) \\
&= q \cdot \mathbb{P}_q(\mathbf{1}(e) = 1) + \mathbb{P}_q\big(\tilde{\omega}^{(2)}(e) = 1\big) \cdot \mathbb{P}_q(\mathbf{1}(e) = 0) \\
&= q,
\end{aligned}$$

showing that (9) holds for the base case where $|E| = 1$.

Assume that (9) holds for any $E$ with $|E| = k$. Consider the situation where the cylinder set corresponds to $k+1$ edges. For simplicity, we write the cylinder set as $C_+(E \cup \{e\})$, where $E \subset E^{\mathbb{T}}$ contains exactly $k$ edges, and $e \in E^{\mathbb{T}} \setminus E$. By the induction hypothesis,

$$\begin{aligned}
\mathbb{P}_q\big(\omega^{(2)} \in C_+(E \cup \{e\})\big) &= \mathbb{P}_q\big(\omega^{(2)} \in C_+(E \cup \{e\}) \mid \omega^{(2)} \in C_+(E)\big) \cdot \mathbb{P}_q\big(\omega^{(2)} \in C_+(E)\big) \\
&= \mathbb{P}_q\big(\omega^{(2)} \in C_+(E \cup \{e\}) \mid \omega^{(2)} \in C_+(E)\big) \cdot q^{|E|}.
\end{aligned}$$

Using the law of total probability by conditioning on $B_n^{(2)}$ and $B_n^{(3)}$,

$$\begin{aligned}
&\mathbb{P}_q\big(\omega^{(2)}(e) = 1 \mid \omega^{(2)} \in C_+(E), \mathbf{1}(e) = 1\big) \\
&\qquad = \sum_{n=1}^{\infty} \sum_{B} \mathbb{P}_q\big(\omega^{(2)}(e) = 1 \mid \omega^{(2)} \in C_+(E), e \in B_n^{(2)}, B_n^{(3)} = B, \mathbf{1}(e) = 1\big) \\
&\qquad\qquad \cdot \mathbb{P}_q\big(e \in B_n^{(2)}, B_n^{(3)} = B \mid \omega^{(2)} \in C_+(E), \mathbf{1}(e) = 1\big),
\end{aligned}$$

where the last summation is over all $B \subset \mathbb{E}^3 \cdot R$ such that $e \in proj(B)$ and $B \subseteq I[\{v\}]$ for some $v \in \mathbb{Z}^3 \cdot R$. Notice that, given $e \in B_n^{(2)}$ and $B_n^{(3)} = B$, we have $\omega^{(2)}(e) = 1$ if and only if the unique edge in $B$ whose projection is $e$ is open under configuration $\omega^{(3)}$. This event occurs with probability $q$ and is independent of $\{\omega^{(2)} \in C_+(E)\}$. Thus,

$$\begin{aligned}
&\mathbb{P}_q\big(\omega^{(2)}(e) = 1 \mid \omega^{(2)} \in C_+(E), \mathbf{1}(e) = 1\big) \\
&\qquad = q \cdot \sum_{n=1}^{\infty} \sum_{B} \mathbb{P}_q\big(e \in B_n^{(2)}, B_n^{(3)} = B \mid \omega^{(2)} \in C_+(E), \mathbf{1}(e) = 1\big) \\
&\qquad = q.
\end{aligned}$$

Consequently,

$$\begin{aligned}
&\mathbb{P}_q\big(\omega^{(2)} \in C_+(E \cup \{e\}) \mid \omega^{(2)} \in C_+(E)\big) \\
&\qquad = \mathbb{P}_q\big(\omega^{(2)}(e) = 1 \mid \omega^{(2)} \in C_+(E), \mathbf{1}(e) = 1\big) \cdot \mathbb{P}_q\big(\mathbf{1}(e) = 1 \mid \omega^{(2)} \in C_+(E)\big) \\
&\qquad\quad + \mathbb{P}_q\big(\omega^{(2)}(e) = 1 \mid \omega^{(2)} \in C_+(E), \mathbf{1}(e) = 0\big) \cdot \mathbb{P}_q\big(\mathbf{1}(e) = 0 \mid \omega^{(2)} \in C_+(E)\big) \\
&\qquad = q \cdot \mathbb{P}_q\big(\mathbf{1}(e) = 1 \mid \omega^{(2)} \in C_+(E)\big) + q \cdot \mathbb{P}_q\big(\mathbf{1}(e) = 0 \mid \omega^{(2)} \in C_+(E)\big) \\
&\qquad = q.
\end{aligned}$$

In summary, we have $\mathbb{P}_q(\omega^{(2)} \in C_+(E \cup \{e\})) = q^{|E|} \cdot q = q^{|E|+1}$. Using induction, (9) holds for any $E \subset E^{\mathbb{T}}$, $|E| < \infty$, and the proof is complete.

https://doi.org/10.1017/jpr.2020.111 Published online by Cambridge University Press

## References


[1] ADLER, J. (1984). A second look at a controversial percolation exponent – Is $\eta$ negative in three dimensions? *Z. Phys. B* **55**, 227–229.

[2] ARGOLO, C., TENORIO, V. AND LYRA, M. L. (2019). Stationary and dynamical critical behavior of the three-dimensional diffusive epidemic process. *Physica A* **517**, 422–430.

[3] BENJAMINI, I. AND SCHRAMM, O. (1996). Percolation beyond $\mathbb{Z}^d$, many questions and a few answers. *Electron. Commun. Prob.* **1**, 71–82.

[4] BOLLOBÁS, B. AND RIORDAN, O. (2006). *Percolation*. Cambridge University Press.

[5] BROADBENT, S. R. AND HAMMERSLEY, J. M. (1957). Percolation processes. *Math. Proc. Camb. Phil. Soc.* **53**, 629–641.

[6] CAMPANINO, M. AND RUSSO, L. (1985). An upper bound on the critical percolation probability for the three-dimensional cubic lattice. *Ann. Prob.* **13**, 478–491.

[7] COTAR, C., HOLROYD, A. E. AND REVELLE, D. (2009). A percolating hard sphere model. *Random Structures Algorithms* **34**, 285–299.

[8] DAMMER, S. M. AND HINRICHSEN H. (2004). Spreading with immunization in high dimensions. *J. Statist. Mech.* **2004**, P07011.

[9] DAMRON, M., HANSON, J. AND SOSOE, P. (2017). On the chemical distance in critical percolation. *Electron. J. Prob.* **22**, 75.

[10] DE MAGALHÃES, A. C., TSALLIS, C. AND SCHWACHHEIM, G. (1980). Probability renormalisation group treatment of bond percolation in square, cubic and hypercubic lattices. *J. Phys. C* **13**, 321–330.

[11] DOH, J., PARK, S. I., YANG, Q. AND RAGHAVAN, N. (2019). The effect of carbon nanotube chirality on the electrical conductivity of polymer nanocomposites considering tunneling resistance. *Nanotechnology* **30**, 465701.

[12] DON, H. (2015). New methods to bound the critical probability in fractal percolation. *Random Structures Algorithms* **47**, 710–730.

[13] DONG, S., WU, X., WANG, E. H. AND WANG, X. J. (2019). Reduced percolation threshold of multi-walled carbon nanotubes/polymer composites by filling aligned ferromagnetic particles. *J. Intell. Mater. Syst. Struct.* **31**, 187–197.

[14] GAUNT, D. S. AND SYKES, M. F. (1983). Series study of random percolation in three dimensions. *J. Phys. A* **16**, 783–799.

[15] GRASSBERGER, P. (1986). Surface and edge exponents for the spreading of 3D percolation. *J. Phys. A* **19**, L241–L246.

[16] GRASSBERGER, P. (1992). Numerical studies of critical percolation in three dimensions. *J. Phys. A* **25**, 5867–5888.

[17] GRIMMETT, G. R. (1999). *Percolation*. Springer, New York.

[18] GRIMMETT, G. R. AND MANOLESCU, I. (2013). Inhomogeneous bond percolation on square, triangular and hexagonal lattices. *Ann. Prob.* **41**, 2990–3025.

[19] GRIMMETT, G. R. AND MANOLESCU, I. (2014). Bond percolation on isoradial graphs: Criticality and universality. *Prob. Theory Relat. Fields* **159**, 273–327.

[20] HEERMANN, D. W. AND STAUFFER, D. (1981). Phase diagram for three-dimensional correlated site-bond percolation. *Z. Phys. B* **44**, 339–344.

[21] HUGHES, B. D. (1995). *Random Walks and Random Environments*, Vol. **2**. Oxford University Press.

[22] KALLIKRAGAS, D. T. AND SVISHCHEV, I. M. (2019). Percolation transitions of physically and hydrogen bonded clusters in supercritical water. *J. Molec. Liq.* **290**, 111213.

[23] KESTEN, H. (1980). The critical probability of bond percolation on the square lattice equals 1/2. *Commun. Math. Phys.* **74**, 41–59.

[24] KESTEN, H. (1982). *Percolation Theory for Mathematicians.* Birkhäuser, Boston.

[25] LIN, J. J., ZHANG, W. L., CHEN, H. S., ZHANG, R. L. AND LIU, L. (2019). Effect of pore characteristic on the percolation threshold and diffusivity of porous media comprising overlapping concave-shaped pores. *Int. J. Heat Mass Transfer* **138**, 1333–1345.

[26] LORENZ, C. D. AND ZIFF, R.M. (1998). Precise determination of the bond percolation thresholds and finite-size scaling corrections for the SC, FCC, and BCC lattices. *Phys. Rev. E* **57**, 230–236.

[27] MAY, W. D. AND WIERMAN, J. C. (2003). Recent improvements to the substitution method for bounding percolation thresholds. *Congr. Numer.* **162**, 5–26.

[28] MAY, W. D. AND WIERMAN, J. C. (2005). Using symmetry to improve percolation threshold bounds. *Combinatorics Prob. Comput.* **14**, 549–566.

[29] MEN'SHIKOV, M. V. AND PELIKH K.D. (1989). Percolation with several defect types. An estimate of critical probability for a square lattice. *Math. Notes* **46**, 778–785.


https://doi.org/10.1017/jpr.2020.111 Published online by Cambridge University Press

[30] ODAGAKI, T. AND CHANG, K. C. (1984). Real-space renormalization-group analysis of quantum percolation. *Phys. Rev. B* **30**, 1612–1614.

[31] PAN, Z. C., WANG, D. L., MA, R. J. AND CHEN, A. R. (2018). A study on ITZ percolation threshold in mortar with ellipsoidal aggregate particles. *Comput. Concr.* **22**, 551–561.

[32] SAHIMI, M., HUGHES, B. D., SCRIVEN, L. E. AND DAVIS, H. T. (1983). Real-space renormalization and effective-medium approximation to the percolation conduction problem. *Phys. Rev. B* **28**, 307–311.

[33] SCHRAM, R. D., BARKEMA, G. T. AND BISSELING, R. H. (2011). Exact enumeration of self-avoiding walks. *J. Statist. Mech. Theory Exp.* **2011**, P06019.

[34] STAUFFER, D., ADLER, J. AND AHARONY, A. (1994). Universality at the three-dimensional percolation threshold. *J. Phys. A* **27**, L475–L480.

[35] STAUFFER, D. AND ZABOLITZKY, J. G. (1986). Re-examination of 3D percolation threshold estimates. *J. Phys. A* **19**, 3705–3706.

[36] SYKES, M. F. AND ESSAM, J. W. (1964). Exact critical percolation probabilities for site and bond problems in two dimensions. *J. Math. Phys.* **5**, 1117–1127.

[37] TSALLIS, C. (1982). Phase diagram of anisotropic planar Potts ferromagnets: A new conjecture. *J. Phys. C* **15**, L757–L764.

[38] VAN DEN BERG, J. AND ERMAKOV, A. (1996). A new lower bound for the critical probability of site percolation on the square lattice. *Rand. Struct. Algorithms* **8**, 199–212.

[39] VAN DER MARCK, S. C. (1997). Percolation thresholds and universal formulas. *Phys. Rev. E* **55**, 1514–1517.

[40] VYSSOTSKY, V. A., GORDON, S. B., FRISCH, H. L. AND HAMMERSLEY, J. M. (1961). Critical percolation probabilities (bond problem). *Phys. Rev.* **123**, 1566–1567.

[41] WANG, J., ZHOU, Z., ZHANG, W., GARONI, T. M. AND DENG, Y. (2013). Bond and site percolation in three dimensions. *Phys. Rev. E* **87**, 052107.

[42] WIERMAN, J. C. (1981). Bond percolation on honeycomb and triangular lattices. *Adv. Appl. Prob.* **13**, 293–313.

[43] WIERMAN, J. C. (1990). Bond percolation critical probability bounds for the kagomé lattice by a substitution method. In *Disorder in Physical Systems,* eds G. GRIMMETT AND D. WELSH. Oxford University Press, pp. 349–360.

[44] WIERMAN, J. C. (1995). Substitution method critical probability bounds for the square lattice site percolation model. *Combinatorics Prob. Comput.* **4**, 181–188.

[45] WIERMAN, J. C. (2002). Bond percolation critical probability bounds for three Archimedean lattices. *Rand. Struct. Algorithms* **20**, 507–518.

[46] WIERMAN, J. C. (2003). Upper and lower bounds for the kagome lattice bond percolation critical probability. *Combinatorics Prob. Comput.* **12**, 95–111.

[47] WIERMAN, J. C. (2015). An improved upper bound for the bond percolation threshold of the cubic lattice. In *Proc. 2015 Joint Statistics Meetings*. American Statistical Association.

[48] WIERMAN, J. C. (2016). Tight bounds for the bond percolation threshold of the $(3, 12^2)$ lattice. *J. Phys. A* **49**, 475002.

[49] WIERMAN, J. C. AND ZIFF, R. M. (2011). Self-dual planar hypergraphs and exact bond percolation thresholds. *Electron. J. Combinatorics* **18**, 61–80.

[50] WIERMAN, J. C., YU, G. AND HUANG, T. (2015). A disproof of Tsallis' bond percolation threshold conjecture for the kagome lattice. *Electron. J. Combinatorics* **22**, P2.52.

[51] WILKE, S. (1983). Bond percolation threshold in the simple cubic lattice. *Phys. Lett. A* **96**, 344–346.

[52] YU, G. (2018). Rigorous bounds for bond percolation thresholds of three-dimensional lattices. Doctoral dissertation. Johns Hopkins University, Baltimore.

[53] ZIFF, R. M. (2006). Generalized cell–dual-cell transformation and exact thresholds for percolation. *Phys. Rev. E* **73**, 016134.

[54] ZIFF, R. M. AND SCULLARD, C. R. (2006). Exact bond percolation thresholds in two dimensions. *J. Phys. A* **39**, 15083.

[55] ZIFF, R. M., SCULLARD, C. R., WIERMAN, J. C. AND SEDLOCK, M. R. (2012). The critical manifolds of inhomogeneous bond percolation on bow-tie and checkerboard lattices. *J. Phys. A* **45**, 494005.


https://doi.org/10.1017/jpr.2020.111 Published online by Cambridge University Press